Journal of Cellular Biochemistry 81:295–303 (2001)

Inhibition Effects of Di(2-Ethylhexyl)Phthalate on Mouse-Liver Lysosomal Vacuolar H^+-ATPase

Tao Wang, Tadayoshi Uezato, and Naoyuki Miura*

Department of Biochemistry, Hamamatsu University School of Medicine, Hamamatsu 431-3192, Japan

Abstract We investigated the effects of di(2-ethylhexyl)phthalate (DEHP) on mouse-liver lysosomes. After 2 weeks of oral administration in mice, a reduction in vacuolar H^+-ATPase (V-ATPase) was observed, and after 3 weeks, the liver lysosomal compartment was completely negative for V-ATPase, as determined by immunocytochemical analysis. When the mice were subsequently fed a normal diet for 1 week, V-ATPase levels recovered to normal values. According to Northern blot analysis, V-ATPase subunit A mRNA decreased gradually with DEHP treatment. Enzyme cytochemical staining showed acid phosphatase (AcPase) to be present in lysosomes and late autophagosomes (autolysosomes) in normal animals as well as in DEHP-treated animals. But the number of late autophagosomes containing AcPase increased clearly after DEHP treatment. These results suggest that: (1) DEHP causes marked V-ATPase reduction in the liver lysosomal compartment and the effect of DEHP is reversible; and (2) the effect of DEHP on protein expression is likely to be exerted at the transcriptional level. J. Cell. Biochem. 81:295–303, 2001. © 2001 Wiley-Liss, Inc.

Key words: V-ATPase; DEHP; acid phosphatase; autophagosome; lysosome

It is well established that hypolipidemic drugs [Hess et al., 1965; Leighton et al., 1975; Fahimi et al., 1982] and other chemicals can inhibit fatty acid metabolism and induce proliferation of peroxisomes and mitochondria [Reddy and Krishnakantha, 1975; Yokota, 1986a; Ganning et al., 1989; Kalen et al., 1990; Winberg and Badr, 1995]. Rat-liver peroxisomes have been shown to markedly increase in number in response to administration of di(2-ethylhexyl)phthalate (DEHP) for 2 weeks, and the number and size of the peroxisomes recover to normal with a return to normal diet [Yokota, 1986b]. When leupeptin is injected into DEHP-pretreated rats, there is a marked accumulation of autophagosomes containing excess cell organelles in the hepatocytes. Using this as an experimental model, the early stage of autophagosome formation has been analyzed by electron microscopy, and it has been suggested that excess peroxisomes are degraded by the autophagic system [Yokota, 1993a, 1993b]. Although the proliferation of peroxisomes induced by DEHP has been investigated, questions concerning the accumulation of other cell organelles remain unanswered so far.

Vacuolar H^+-ATPase (V-ATPase) is localized in organelles of the central vacuolar system such as lysosomes, coated vesicles, and the Golgi apparatus, and it plays an important role in maintaining the acidic environment in these compartments [Mellman et al., 1986; Moriyama, 1992; Forgac, 1992, 1999]. The acidic environment is the key to the activity of digestive enzymes [Munn, 1994], and may be important for the fusion of lysosomes with autophagosomes [Klionsky, 1992; Yamamoto, 1998]. Subunit A is thought to be the main component of the ATP binding site and catalytic domain of V-ATPase [Pan et al., 1991; Van Hille et al., 1993, 1995]. Previously, reports showed that early autophagosomes obtain lysosomal enzymes by fusion with lysosomal compartments including late endosomes and that excess peroxisomes and mitochondria trapped in autophagosomes may be degraded by

Grant sponsor: Ministry of Education, Science, Sports and Culture of Japan.

*Correspondence to: Naoyuki Miura, Department of Biochemistry, Hamamatsu University School of Medicine, 3600 Handa-cho, Hamamatsu, 431-3192, Japan.
E-mail: nmiura@hama-med.ac.jp

Received 14 August 2000; Accepted 4 October 2000

these digestive enzymes [Yokota, 1993a, b, 1995]. However, the precise mechanism whereby excess cell organelles are induced by DEHP has not been investigated. In this study, we report that DEHP treatment causes a reduction in V-ATPase subunit A in the liver lysosomal compartment, which may account for the inability to degrade excess cell organelles.

MATERIALS AND METHODS

Treatment of Animals

C3H mice weighing 25–30 g were used. The animals were fed a 2% DEHP (Wako Pure Chemicals, Tokyo, Japan) containing laboratory diet or a normal diet for 3 weeks [Shindo et al., 1978]. To observe recovery of V-ATPase following its inhibition, the animals were subsequently fed a normal diet. After overnight fasting, the animals were sacrificed and liver specimens were fixed and then cut into smaller pieces. The fixative consisted of 2% glutaraldehyde, 0.1 M cacodylate buffer (pH 7.4), 0.01% $CaCl_2$, and 5% sucrose. After several washes in cacodylate buffer, the tissue was processed in LR White (London Rein, Hampshire, UK) embedding medium for postembedding immunocytochemistry or Epon (Taab, London, UK) embedding medium for immunoenzyme histochemistry.

Antibodies

Polyclonal antibodies against V-ATPase subunit A were generated as described previously [Sudhof et al., 1989; Mattsson et al., 1994; Moriyama and Yamamoto, 1995; Moriyama et al., 1995]. Antibodies were raised in New Zealand White rabbits against a synthetic peptide (AEMPADSGYPAYLGAR; residues 367–382 of V-ATPase subunit A). The peptide was conjugated with keyhole limpet haemocyanin (KLH) according to the instructions of the Pierce antibody production kit (Pierce, Rockford, IL). m-Maleimidobenzoyl-*N*-hydroxy-succinimide ester (MBS) was used for coupling. Two rabbits were injected intramuscularly with 100 μg of synthetic peptide coupled to carrier and emulsified in complete Freund's adjuvant. Subsequent injections at days 14 and 28 were performed in incomplete Freund's adjuvant. Antibodies that recognized the V-ATPase subunit A were purified from antiserum using affinity columns with peptide-conjugated Sepharose.

Immunoblot Analysis

Liver tissues (0.5 g) from DEHP-treated and untreated mice were homogenized in 5 ml of 0.01 M potassium phosphate buffer (pH 7.0) containing a cocktail of five different proteinase inhibitors as described previously [Yokota, 1990]. The homogenates were fractionated, and mitochondrial and microsomal fractions were subjected to sucrose density gradient centrifugation. The lysosomal membrane-rich fractions were recovered at the 40/50% interface. These samples were mixed with the same volume of Laemmli sample buffer [Laemmli, 1970] and boiled for 3 min. Electrophoresis was carried out on a 9% SDS-polyacrylamide gel. Proteins in the gel were transferred to nitrocellulose sheets (Amersham, Arlington Heights, IL), blocked in 5% MPBST (comprising 5% nonfat milk powder and 0.1% Tween 20 in phosphate-buffered saline, PBS) at room temperature for 1 h, and then the immunoblots were incubated with a 1:200 dilution of anti-V-ATPase antibody. After extensive washing in PBS (containing 0.1% Tween-20), anti-rabbit IgG antibody conjugated to horseradish peroxidase (HRP) was added, and the membranes were incubated for 1 h at room temperature. Protein antigens were detected by chemiluminescence using an electroluminescent (ECL) detection system (Amersham) followed by exposure to X-ray film (Fuji Film, Tokyo, Japan).

Immunofluorescence Staining

All fixation and staining procedures were conducted at room temperature. The tyramide signal amplification (TSA) kit used for immunofluorescence staining was obtained from NEN Life Science Products (Boston, MA). The tissues were fixed in 10% formalin and embedded in paraffin. Semithin sections (4 μm) were cut using a LEICA RM2135 rotary microtome. Sections mounted on glass slides were stained using the TSA technique of Fabienne [1998]. Briefly, semithin sections were deparaffinized and preincubated with 10% normal goat serum (NGS; Lab-Systems, Aidenbach, Germany) for 20 min. This was followed by a 3-hour incubation with primary antibody diluted in 10% NGS. Three washes in Tris–saline were followed by treatment with biotinylated goat anti-rabbit IgG antibody (diluted 1:500 in Tris–saline containing 4% NGS and 0.05% Triton X-100). After washing three times for 10 min with

TNT buffer (0.1 M Tris–HCl, pH 7.5, 0.15 M NaCl, 0.05% Tween-20), the sections were blocked with TNB buffer (0.1 M Tris–HCl, pH 7.5, 0.15 M NaCl, 0.5% NEN blocking reagent) for 30 min. They were then incubated for 30 min with a 1:2000 streptavidin-HRP dilution in TNB. After washing three times for 10 min with TNT, the sections were incubated with biotinylated tyramide in amplification diluent for 5 min. Thereafter, the sections were rinsed three times for 10 min in TNT and then TNB. They were then incubated for 30 min in streptavidin-fluorescein (diluted 1:1000 in TNB). Finally, the sections were washed three times for 10 min with PBS, dehydrated, and coverslipped.

Immunoelectron Microscopy

Liver tissue prefixed and washed as described above was cut into 300-μm sections with a Vibratome and embedded in LR White medium. The resin was cured with LR White accelerator (1 drop/8 ml) at 4°C. This caused polymerization between 10 and 20 min. Thin sections were cut with a LEICA ultracut microtome equipped with a diamond knife and mounted on nickel grids. Immunogold staining of the sections was based on the procedures described by Roth [1982]. Briefly, thin sections mounted on the grids were treated with 1% bovine serum albumin (BSA) in PBS for 15 min and then incubated with V-ATPase antibodies (10–20 μg/ml) overnight at 4°C. Fifteen nanometer gold-conjugated goat anti-rabbit IgG antibodies (BioCell, Cardiff, UK) were diluted 1:50 in 1% BSA/PBS. In the absence of the primary antibody, the anti-rabbit IgG antibodies did not react with liver cells. After washing with PBS, the sections were incubated with the gold-labeled secondary antibodies for 30 min. The sections were then washed with distilled water, air-dried, contrasted with 2% uranyl acetate for 5 min and with lead citrate for 3 min and examined in a JEM-1220 electron microscope at an accelerating voltage of 80 kV.

Enzyme Cytochemistry

Fixed liver tissue blocks were cut into 50-μm sections and further fixed with 2% glutaraldehyde in 0.1 M cacodylate buffer (pH 7.4) for 1 h at 4°C. After fixation, the sections were washed thoroughly with physiological saline and incubated with a cerium reaction medium for acid phosphatase [Robinson et al., 1983] containing 1 mM β-glycerophosphate, 2 mM $CeCl_3$, and 0.1 M acetate buffer (pH 5.0). The sections were incubated for 1 h at 37°C, with the medium being replaced with freshly prepared medium after 30 min. After incubation, the sections were washed three times in 0.1 M cacodylate buffer (pH 7.2) containing 5% sucrose. The tissue sections were refixed in 3% glutaraldehyde–0.1 M cacodylate buffer (pH 7.2) for 1 h, washed overnight at 4°C in the same buffer and then were treated with 2% O_SO_4–0.1 M cacodylate (pH 7.2) for 1 h at room temperature. The sections were then dehydrated in a graded ethanol series and embedded in Epon. For electron microscopic observation, ultrathin sections were cut with a diamond knife and stained with uranyl acetate and lead citrate. The sections were examined using a JEM-1220 electron microscope at an accelerating voltage of 80 kV.

Northern Blot Analysis

Total RNA from mouse liver was extracted using Isogen (Nippon Gene, Osaka, Japan). For Northern blots, RNA (15 μg) was separated on 1.0% agarose gels containing 2.2 M formaldehyde and transferred to nylon membranes (Hybond N, Amersham). Prehybridization was carried out in 5 × saline–sodium citrate (SSC), 5 × Denhardt's solution, 25 mM sodium phosphate, pH 6.4, 0.1% sodium dodecylsulfate (SDS), 250 μg/ml sonicated denatured herring sperm DNA, 25 μg/ml poly(A), and 50% formamide at 42°C for 4 h. For hybridization, 20% dextran sulfate and appropriate [^{32}P]-labeled cDNA probes (nucleotides 1385–1913 of V-ATPase subunit A mRNA) were included. The membrane was washed twice in 2 × SSC and 0.1% SDS for 15 min at room temperature and twice in 1 × SSC and 0.1% SDS for 15 min at 45°C. The radioactivity on the membrane was measured by a BAS 1000 Fuji bioimaging analyzer (Fuji Film, Tokyo, Japan).

RESULTS

Antibodies Specifically Recognized V-ATPase Subunit A

First of all, we investigated whether the purified antibodies specifically recognized V-ATPase. Western blot analysis reveals that a single band of 69 kDa was detected in the total liver homogenate and the lysosomal fraction,

but not in the nuclear fraction (Fig. 1A). The estimated size of the band is in good agreement with that of V-ATPase subunit A. For confirming the specificity of the antibodies, we incubated the transferred nitrocellulose membrane with the antibodies in the presence of the antigen peptide. The 69 kDa band disappeared when the peptide was present (Fig. 1B, lane 1). These results show that the purified antibodies specifically recognized V-ATPase subunit A.

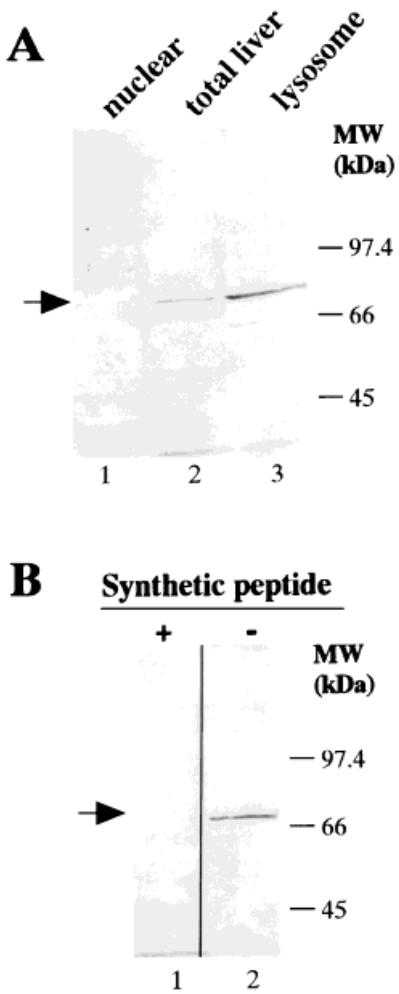

Fig. 1. The antibodies specifically recognize V-ATPase subunit A. **A: Lane 1**, cell nuclear fraction (20 μg); **lane 2**, total liver homogenate (30 μg); **lane 3**, purified lysosomal fraction (8 μg). Samples were subjected to SDS polyacrylamide gel electrophoresis and electrophoretically transferred to nitrocellulose as described under Materials and Methods. Rabbit polyclonal antibodies generated against the 69-kDa subunit of V-ATPase were used for Western blotting, as described under Materials and methods **B**: Western blot analysis of purified lysosomal fraction with purified polyclonal antibodies in the presence (**lane 1**) and absence (**lane 2**) of the peptide.

Inhibition of V-ATPase by DEHP

Since V-ATPase is a key enzyme in the lysosomal compartment, we investigated the effect of DEHP on this enzyme (Fig. 2). The levels of V-ATPase decreased gradually during DEHP treatment, and after 3 weeks it almost completely disappeared (lane 4). We also investigated these changes by indirect immunofluorescence staining of V-ATPase in the liver. Consistent with immunoblot analysis, intense V-ATPase fluorescence was apparent in normal liver cells (Fig. 3A), but the fluorescence intensity of V-ATPase was greatly diminished after DEHP treatment (Fig. 3B). Thin sections of LR White-embedded normal liver tissue were also stained for the same antigen by immunogold. Gold particles indicating V-ATPase immunoreactivity were present on lysosomal membranes (Fig. 4). During DEHP treatment this labeling became negative with time (data not shown). These results clearly demonstrate that administration of DEHP causes marked V-ATPase subunit A inhibition in the mouse-liver lysosomal compartment.

Effect of DEHP on V-ATPase mRNA Levels in Mouse Liver

To determine if the reduction of V-ATPase subunit A protein is due to a decrease in gene expression, the expression of the V-ATPase gene was investigated by measuring V-ATPase subunit A mRNA levels in mouse liver. Northern blot analysis of total RNA obtained from the livers of untreated or DEHP-treated mice is shown in Figure 5. The cDNA probe for V-

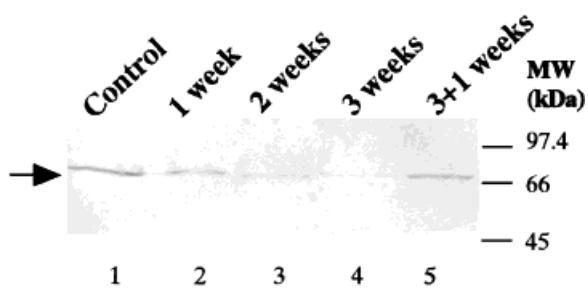

Fig. 2. Immunoblot analysis of lysosomal fractions from mouse livers treated with DEHP. The samples were analyzed by Western blotting with an antibody against the 69-kDa A subunit of V-ATPase. The treatments were as follows: control (**lane 1**), DEHP-treated for 1 week (**lane 2**), 2 weeks (**lane 3**) and 3 weeks (**lane 4**); and normal diet for 1 week after 3 weeks of DEHP loading (**lane 5**). The molecular weight of standard markers is indicated at the right; 97.4 kDa (phosphorylase B), 66 kDa (BSA), 45 kDa (egg albumin).

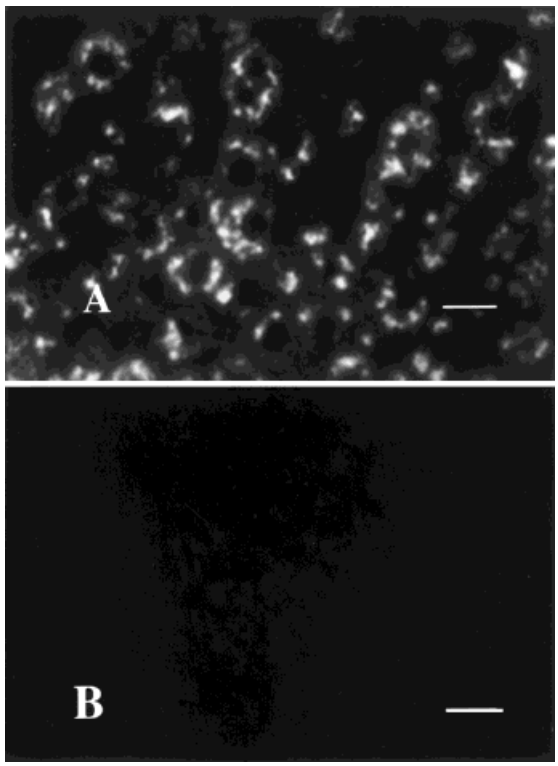

Fig. 3. Indirect immunofluorescence staining of V-ATPase in the liver of control and DEHP-treated mice. The tissues were fixed and stained with affinity-purified V-ATPase antibodies that recognize V-ATPase subunit A. **A**: Untreated control. The immunofluorescence signal is observed in the liver section. **B**: DEHP treatment for 3 weeks. The immunofluorescence signal is very weak. Bars, 60 μm.

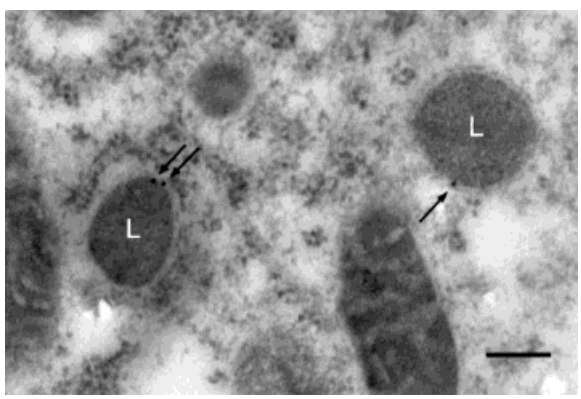

Fig. 4. Electron microscopic localization of V-ATPase in hepatocytes from an untreated mouse. Gold particles are localized in the lysosomal membranes (arrows). Bars, 200 nm.

ATPase subunit A recognized a 3.4-kb band (lane 1). This signal decreased with DEHP treatment (lanes 2–4). The decrease in mRNA was consistent with the decrease in the corresponding protein level. The close relationship

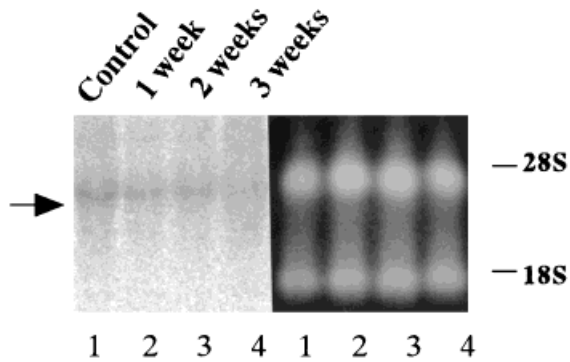

Fig. 5. Northern blot analysis of V-ATPase mRNA obtained from control and DEHP-treated mice. Left: Total RNA (15 μg) was subjected to Northern analysis using [^{32}P]-labeled cDNA probes for V-ATPase subunit A. The positions of the 28 and 18 S ribosomal bands are indicated on the right. **Lane 1**: control; **lane 2**: DEHP treatment for 1 week; **lane 3**: DEHP treatment for 2 weeks; **lane 4**: DEHP treatment for 3 weeks. Right: Ethidium bromide staining of the same gel demonstrating equal loading.

between the treatment-associated decreases in V-ATPase protein and mRNA levels suggests that the effect of DEHP on V-ATPase protein expression is exerted mainly at the transcriptional level.

Recovery From Inhibition

To test whether the effect of DEHP is reversible, we analyzed cell fractions using the immunoblot method. Western blot analysis of liver homogenates showed that the signal for immunoreactive V-ATPase decreased only slightly during the first week of DEHP treatment and then decreased further during the second week. After 3 weeks, the signal almost completely disappeared. When DEHP was subsequently removed from the diet, the signal gradually increased, and 1 week after removal of DEHP, the signal returned to the level seen in untreated mice (Fig. 2, lane 5). These results show clearly that the effect of DEHP is reversible. Similar results were obtained with indirect immunofluorescence staining of V-ATPase (data not shown).

Enzyme Cytochemical Analysis of the Fusion of the Lysosomal Compartment With Autophagosomes

Autophagosomes acquire acid hydrolase by fusion with lysosomes [Dunn, 1990, 1994; Yokota, 1995]. Acid phosphatase (AcPase) is localized to lysosomal compartments [Novikoff, 1987]. We determined the localization of AcPase to study the effect of DEHP on the

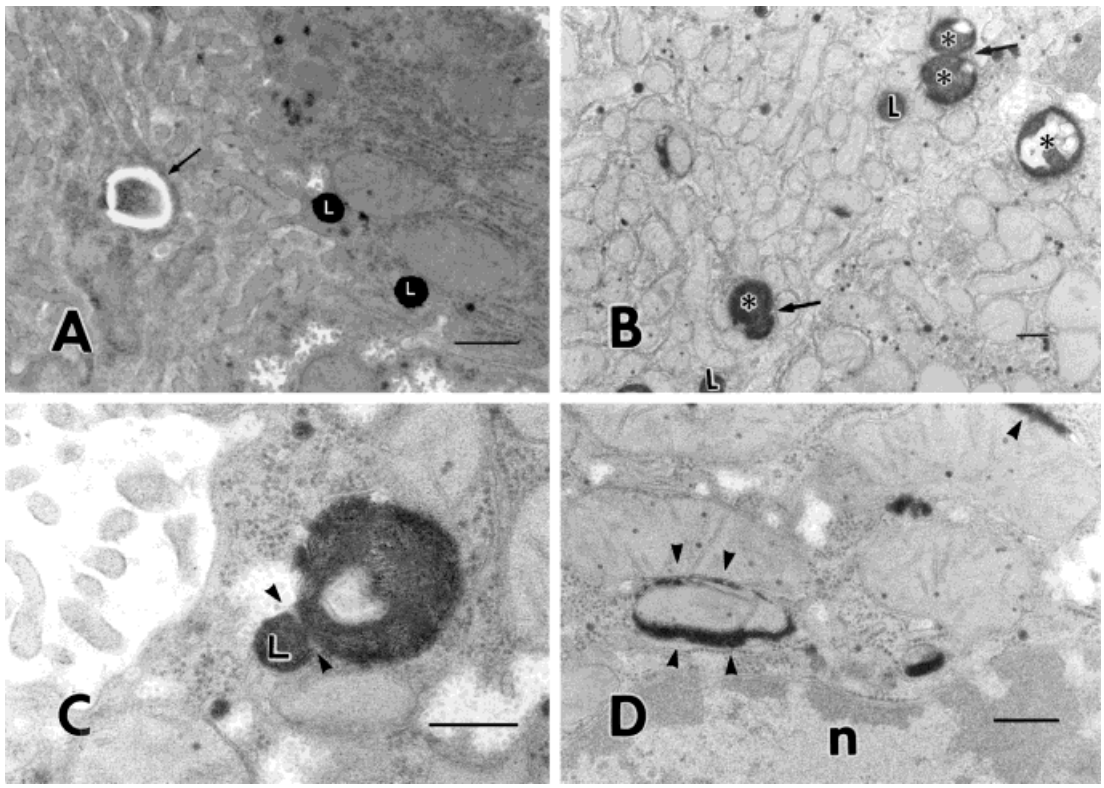

Fig. 6. Acid phosphatase staining in early to late autophagic vacuoles. Liver tissues were obtained from control mice and mice treated with DEHP for 3 weeks. **A**: Untreated control. An acid phosphatase–negative early autophagosome (arrow) and acid phosphatase–positive lysosomes (L) are seen. Note that electron-dense reaction product completely fills the lysosomes. Bars, 500 nm. **B**: DEHP-treated. Reaction deposits are present in lysosomes (L) and excess late autophagosomes (asterisks). Because late autophagosomes contain cell organelle fractions, acid phosphatase reaction product does not completely fill their interior. Some autophagosomes fuse with each other (arrows). Bars, 500 nm. **C**: DEHP-treated. Fusion between a reaction-positive lysosome and a late autophagic vacuole is also seen (arrowheads). Bars, 200 nm. **D**: DEHP-treated. A reaction-positive autophagic vacuole enclosing a mitochondrion is observed (arrowheads). Bars, 200 nm.

fusion process. For this purpose, we observed acid–phosphatase reaction product in the cytoplasm by electron microscopy after enzyme cytochemical staining. In control and DEHP-treated hepatocytes, the reaction product was found in lysosomes and late autophagosomes, and the fusion between lysosomes and autophagosomes that encloses the cytoplasmic matrix was observed frequently (Fig. 6). As late autophagosomes contain cell organelle fractions, AcPase reaction product does not completely fill its interior. In contrast, electron-dense reaction product completely fills lysosomes. Thus, these two cell organelles are distinguishable from each other [Novikoff, 1982; Robinson and Karnovsky, 1983; Miharu et al., 1997; Yamamoto, 1998]. Figure 7 shows the kinetics of the appearance of early and late autophagosomes in DEHP-treated mouse liver. The area percent occupied by autophagosomes

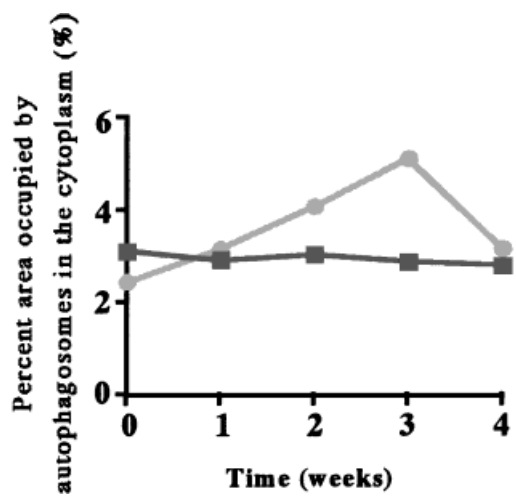

Fig. 7. Kinetics of the appearance of early and late autophagosomes in DEHP-treated mouse liver. Areas with early autophagosomes (■) or late autophagosomes (●) were measured on electron micrographs and plotted as the percentage of autophagosome areas in the cytoplasm over time.

was measured on electron micrographs. The number of late autophagosomes, which contained AcPase reaction deposits, increased dramatically in the cytoplasm after DEHP treatment (Fig. 6B). This excess of late autophagosomes decreased rapidly after removal of DEHP to a level nearly identical to the normal level after 1 week. The number of early autophagosomes, which were not stained by AcPase, was not altered. These results show that DEHP does not block fusion between lysosomes and early autophagosomes in liver cells. Interestingly, the rate of recovery from excess late autophagosomes was reversely correlated with that of V-ATPase after removal of DEHP from the diet. These results suggest that the excess of late autophagosomes is related directly to the decrease of V-ATPase by DEHP treatment.

DISCUSSION

It is well established that DEHP is a peroxisome-proliferating compound and that its administration to rodents induces a pleiotropic response mediated by peroxisome proliferator-activated receptor-alpha (PPAR alpha) [Peters, 1997]. DEHP can induce a marked proliferation of peroxisomes in hepatocytes [Hess et al., 1965; Leighton et al., 1975; Fahimi et al., 1982], and the excess number rapidly decreases to normal after the removal of DEHP from the diet [Yokota, 1993a, b]. Other studies have shown that high levels of peroxisome proliferation and hepatomegaly are associated with DEHP hepatocarcinogenesis in rodent liver, and that the tumorigenic process may be arrested by the cessation of DEHP treatment, suggesting that extended treatment with the compound acts to promote tumor growth [David, 1999]. Although DEHP has been studied extensively, a number of questions concerning the intracellular degradation of DEHP-induced cell organelles still remain to be solved. There are many reports showing that microsomes and mitochondria increase in number after a 2-week treatment with DEHP [Yokota, 1986a, b; Ganning et al., 1989; Kalen et al., 1990]. Other studies have shown that DEHP treatment causes hepatomegaly, which reverses after removal of DEHP from the diet. With the reduction in liver weight, the number of peroxisomes is also reduced to normal [Yokota, 1993a, b]. Furthermore, it has been reported that treatment with the proteinase inhibitor leupeptin causes marked accumulation of autophagosomes in hepatocytes. This accumulation of autophagic vacuoles seems to result from the inhibition of intralysosomal proteolysis by leupeptin [Ishikawa et al., 1983]. When leupeptin was injected into animals pretreated with DEHP, autophagosomes containing numerous peroxisomes and mitochondria accumulated in hepatocytes. Some groups have demonstrated that the process of degradation of excess peroxisomes is carried out by the autophagic system [Yokota, 1993a, b]. Extensive studies have shown the acidification of the luminal space of autophagosomes or lysosomes by V-ATPase to be a key event in cellular autophagy [Munn, 1994; Yamamoto, 1998].

In view of these facts, we hypothesize that the autophagic system, including the lysosomal system, is partially destroyed by DEHP such that it cannot rapidly degrade enclosed cell organelles. This results in an increase in late autophagosomes and liver weight, and induces the proliferation of peroxisomes. To clarify the role of DEHP on the process of intracellular degradation of excess peroxisomes, we determined if late autophagosomes lack lysosomal enzymes after DEHP treatment. For this purpose, we localized the activity of acid phosphatase, a lysosomal enzyme marker, by electron microscopy. Compared with that of controls, AcPase localization did not change in lysosomes or late autophagosomes after DEHP treatment, and fusion between lysosomes and late autophagosomes was observed frequently. These results suggest that DEHP does not prevent the delivery of lysosomal enzymes to autophagosomes. Therefore, we focused on the key enzyme that maintains acidification of the luminal space of autophagosomes and lysosomes and which is important for maximal activity of lysosomal digestive enzymes [Novikoff, 1990].

In this study, we examined the effect of DEHP on lysosomal V-ATPase using immunocytochemical and enzyme cytochemical methods. The results showed that V-ATPase in the lysosomal compartment decreased after treatment with DEHP, which might cause a decrease in the activity of lysosomal digestive enzymes. Furthermore, DEHP induced an increase of late but not early autophagosomes (Fig. 7). This increase in autophagosomes could result from the condition that late autophagosomes, which lack an acidic environment, can-

not rapidly digest enclosed organelles to change into residual bodies. In other words, DEHP destroys the key compartment of the autophagic system and, therefore, autophagosomes lose the ability of digesting these cell organelles. In addition, the recovery from excess late autophagosomes was consistent with that of V-ATPase after removal of DEHP from the diet, so this finding supports the abovementioned hypothesis. In this study, it was shown clearly that the process of autophagosome acquisition of lysosomal enzymes by fusion with lysosomes was not blocked. This is consistent with reports obtained using yeast cells [Nakamura et al., 1997]. In yeast cells, treatment with bafilomycin A_1, a specific inhibitor of V-ATPase, or the destruction of the V-ATPase gene was shown to cause inhibition of degradation in the vacuoles, but did not block fusion between autophagosomes and vacuoles. In addition, other groups have reported that the inhibition of acidification by monensin does not prevent the delivery of cathepsin L to autophagosomes in rat fibroblast cells [Punnonen et al., 1992].

The results obtained in this study are similar to those obtained by Yamamoto [1998]. However, there are some differences. For example, Yamamoto reported that AcPase activity is not detected in autophagosomes that accumulate in the presence of bafilomycin A_1, indicating that fusion between autophagosomes and lysosomes is inhibited in the presence of bafilomycin A_1. This discrepancy could be due to differences in experimental conditions or in the drugs employed.

To investigate whether DEHP affects V-ATPase gene expression in liver cells, we determined mRNA levels for the V-ATPase A subunit in livers obtained from untreated and DEHP-treated mice. Northern blot analysis revealed a lower V-ATPase mRNA level in DEHP-treated mice than in control mice. The mechanisms that lead to a reduction in V-ATPase mRNA are unclear. The DEHP-induced decrease in V-ATPase mRNA level could be due to either a decreased gene transcription rate or a reduced mRNA half-life. Taken together, the findings obtained in this study suggest that administration of DEHP causes a series of effects on lysosomal V-ATPase, and that the DEHP-induced inhibition probably occurs at the level of gene transcription. Currently, we speculate that DEHP may disrupt the lysosomal proton pump and induce an increase in internal pH. Therefore, lysosomal digestive enzymes would not be able to degrade excess cell organelles, resulting in a proliferation of peroxisomes and mitochondria. However, we have no direct evidence to support this hypothesis. It has been reported that some peroxisome-proliferating compounds upregulate the synthesis of peroxisomal proteins [Masters, 1996; Lehmann, 1997; David, 1999]. The possibility that similar upregulation of peroxisomal proteins may be induced by DEHP cannot be excluded. Therefore, we think that V-ATPase inhibition is one of the factors that might account for the accumulation of cell organelles. Our hypothesis will be further tested by infecting mouse liver with a recombinant adenovirus harboring an antisense V-ATPase subunit A sequence to block the synthesis of the subunit A protein.

ACKNOWLEDGMENTS

We thank Ms. M. Kohdabashi and Dr. Y-X. Wu for their excellent technical assistance. T. Wang is the recipient of a Tokai Denpun Scholarship.

REFERENCES

David RM, Moore MR, Cifone MA, Finney DC, Guest D. 1999. Chronic peroxisome proliferation and hepatomegaly associated with the hepatocellular tumorigenesis of di(2-ethylhexyl)phthalate and the effects of recovery. Toxicol Sci 50:195–205.

Dunn WA. 1990. Studies on the mechanisms of autophagy: maturation of the autophagic vacuole. J Cell Biol 110: 1935–1945.

Dunn WA. 1994. Autophagy and related mechanisms of lysosome-mediated protein degradation. Trends Cell Biol 4:139–143.

Fabienne L. 1998. A highly sensitive immunofluorescence procedure for analyzing the subcellular distribution of GABA receptor subunits in the human brain. J Histochem Cytochem 46:1129–1139.

Fahimi HD, Renecke A, Sujatta M, Yokota S, Ozel M, Hartig F, Stegmeier K. 1982. The short- and long-term effects of bezafibrate in the rat. Ann NY Acad Sci 386: 111–133.

Forgac M. 1992. Structure, function and regulation of the coated vesicle V-ATPase. J Exp Biol 172:155–169.

Forgac M. 1999. Structure and properties of the vacuolar (H^+)-ATPase. J Biol Chem 274:12951–12954.

Ganning AE, Olsson MJ, Peterson E, Dallner G. 1989. Fatty acid oxidation in hepatic peroxisomes and mitochondria after treatment of rats with di(2-ethylhexyl)phthalate. Pharmacol Toxicol 65:265–268.

Hess R, Staubli W, Riess W. 1965. Nature of the hepatomegalic effect produced by ethyl-chlorophenoxy-isobutylate in the rat. Nature 208:856–858.

Ishikawa T, Furun K, Kato K. 1983. Ultrastructural studies on autolysosomes in rat hepatocytes after leupeptin treatment. Exp Cell Res 144:15–24.

Kalen A, Appelkvist EL, Dallner G. 1990. The effects of inducers of the endoplasmic reticulum, peroxisomes and mitochondria on the amounts and synthesis of ubiquinone in rat liver subcellular membranes. Chem Biol Interact 73:221–234.

Klionsky DJ. 1992. Compartment acidification is required for efficient sorting of proteins to the vacuole in *Saccharomyces cerevisiae*. J Biol Chem 267:3416–3422.

Laemmli UK. 1970. Cleavage of structural proteins during the assembly of the head of bacteriophage T4. Nature 227:680–685.

Lehmann JM, Lenhard JM, Oliver BB, Ringold GM, Kliewer SA. 1997. Peroxisome proliferator-activated receptors alpha and gamma are activated by indomethacin and other nonsteroidal anti-inflammatory drugs. J Biol Chem 272:3406–3410.

Leighton F, Coloma L, Koenig C. 1975. Structure, composition, physical properties, and turnover of proliferated peroxisomes. A study of the tropic effects of Su-13437 on rat liver. J Cell Biol 67:281–309.

Masters C. 1996. Omega-3 fatty acids and the peroxisome. Mol Cell Biochem 165:83–93.

Mellman I, Fuchs R, Helenius A. 1986. Acidification of the endocytic and exocytic pathways. Ann Rev Biochem 55: 663–700.

Miharu K, Tsuyoshi S, Damon C, Herbert N. 1997. Biogenesis and function of lipolysosomes in developing chick hepatocytes. Microsc Rec Tech 39:444–452.

Moriyama Y, Maeda M, Futai M. 1992. The role of V-ATPase in neuronal and endocrine systems. J Exp Biol 172:171–178.

Moriyama Y, Yamamoto A, Yamada H, Tashiro Y, Tomochika K, Takahashi M, Maeda M, Futai M. 1995. Microvesicles isolated from bovine posterior pituitary accumulate norepinephrine. J Biol Chem 270:11424–11429.

Moriyama Y, Yamamoto A. 1995. Microvesicles isolated from bovine pineal gland specifically accumulate L-glutamate. FEBS Lett 367:233–236.

Munn AL. 1994. Endocytosis is required for the growth of vacuolar H^+-ATPase-defective yeast: identification of six new END genes. J Cell Biol 127:373–386.

Nakamura N, Matsuura A, Wada Y, Ohsumi Y. 1997. Acidification of vacuoles is required for autophagic degradation in the yeast, *Saccaromyces cerevisiae*. J Biochem 121:338–344.

Novikoff AB. 1982. Lysosomes. In: Arias I, Popper H, Schachter D, Shafritz DA, editors. The liver: biology and pathobiology, New York: Raven Press, p 9–25.

Pan YX, Xu J, Strasser JE, Howell M, Dean GE. 1991. Structure and expression of subunit A from the bovine chromaffin cell vacuolar ATPase. FEBS Lett 293:89–92.

Peters JM. 1997. Di(2-ethylhexyl)phthalate induces a functional zinc deficiency during pregnancy and teratogenesis that is independent of peroxisome proliferator-activated receptor-alpha. Teratol 56:311–316.

Punnonen EL, Autio S, Marjomaki VS, Reunanen H. 1992. Autophagy, cathepsin L, transport, and acidification in cultured rat fibroblast. J Histochem Cytochem 40:1579–1587.

Reddy JK, Krishnakantha TP. 1975. Hepatic peroxisome proliferation: induction by two novel compounds structurally unrelated to clofibrate. Science 190:787–789.

Robinson JM, Karnovsky MJ. 1983. Ultrastrutural localization of several phosphatases with cerium. J Histochem Cytochem 31:1197–1208.

Roth J. 1982. The protein A-gold (pAg) technique.A quantitative and qualitative approach for antigen localization of thin sections. In: Bullock GR, Petrusz P, editors. Techniques in immunocytochemistry. Vol 1. London: Academic Press, p 108–133.

Shindo Y, Osumi T, Hashimoto T. 1978. Effects of administration of di-(2ethylhexyl)phthalate on rat liver mitochondria. Biochem Pharmacol 27:2683–2688.

Sudhof TC, Fried VA, Stone DK, Johnston PA, Xie XS. 1989. Human endomembrane H^+ pump strongly resembles the ATP-synthetase of *Archaebacteria*. Proc Natl Acad Sci USA 87:6067–6071.

Van Hille B, Richener H, Evans DB, Green JR, Bilbe G. 1993. Identification of two subunit A isoforms of the vacuolar H^+ ATPase in human osteoclastoma. J Biol Chem 268:7075–7080.

Van Hille B, Richener H, Green JR, Bilbe G. 1995. The ubiquitous VA68 isoform of subunit A of the vacuolar H^+-ATPase is highly expressed in human osteoclasts. Biochem Biophys Res Commun 214:1108–1113.

Winberg LD, Badr MZ. 1995. Mechanism of phthalate-induced inhibition of hepatic mitochondrial beta-oxidation. Toxicol Lett 76:63–69.

Yamamoto A. 1998. Bafilomycin A1 prevents maturation of autophagic vacuoles by inhibiting fusion between autophagosomes and lysosomes in rat hepatoma cell line, H-4-11-E cells. Cell Struct Funct 23:33–42.

Yokota S. 1986a. Quantitative immunocytochemical studies on differential induction of serine: pyruvate aminotransferase in mitochondria and peroxisomes of rat liver cells by administration of glucagon or di-(2-ethylhexyl)phthalate. Histochemistry 85:145–155.

Yokota S. 1986b. Non-autophagic degradation of excess peroxisomes induced by administration of di-(2-ethylhexyl)phthalate. Cytochemical and immunoelectron microscopic studies. Proc. XIth International Congress Electron Microscopy, Kyoto, p 2583–2584.

Yokota S. 1990. Cytochemical and immunocytochemical study on the peroxisomes of rat liver after administration of a hypolipidemic drug. MLM-160. Eur J Cell Biol 53: 112–121.

Yokota S. 1993a. Formation of autophagosomes during degradation of excess peroxisomes induced by administration of dioctyl phthalate. Eur J Cell Biol 61:67–80.

Yokota S. 1993b. Formation of autophagosomes during degradation of excess peroxisomes induced by di-(2-ethylhexyl)-phthalate treatment. II. Immunocytochemical analysis of early and late autophagosomes. Eur J Cell Biol 62:372–383.

Yokota S. 1995. Formation of autophagosomes during degradation of excess peroxisomes induced by di-(2-ethylhexyl)-phthalate treatment. III. Fusion of early autophagosomes with lysosomal compartments. Eur J Cell Biol 66:15–24.